

# Higgs CP Violation from Vectorlike Quarks

Chien-Yi Chen,<sup>1</sup> S. Dawson,<sup>1</sup> and Yue Zhang<sup>2</sup>

<sup>1</sup>*Department of Physics, Brookhaven National Laboratory, Upton, N.Y., 11973, U.S.A.*

<sup>2</sup>*Walter Burke Institute for Theoretical Physics,  
California Institute of Technology, Pasadena, CA 91125*

(Dated: July 28, 2015)

## Abstract

We explore CP violating aspects in the Higgs sector of models where new vectorlike quarks carry Yukawa couplings mainly to the third generation quarks of the Standard Model. We point out that in the simplest model, Higgs CP violating interactions only exist in the  $hWW$  channel. At low energy, we find that rare  $B$  decays can place similarly strong constraints as those from electric dipole moments on the source of CP violation. These observations offer a new handle to discriminate from other Higgs CP violating scenarios such as scalar sector extensions of the Standard Model, and imply an interesting future interplay among limits from different experiments.

## I. INTRODUCTION

Now that a Higgs boson has been observed with properties similar to those predicted by the Standard Model (SM), the next critical task is a program of precision measurements of its properties. Studies of the Higgs mass, coupling strengths, and production and decay channels are well advanced. However, less attention has been paid to the possibility of observing CP violation in the Higgs sector and the purpose of the present work is to explore such a possibility.

If the 125 GeV boson is measured to be a mixture of CP even and odd states, it immediately indicates that there must be new physics not far above the electroweak scale. One of the most straightforward ways is to extend the scalar sector of the SM, and the simplest case is the complex version of the 2 Higgs doublet model (C2HDM) [1–6]. The presence of CP violation leads to observable changes in Higgs production and decay rates, as well as contributions to low energy observables such as electric dipole moments [7]. It has also been pointed out that some of the heavy scalar decay channels could be sensitive to CP violation [8], and could be probed at the LHC and future colliders. The complementarity of LHC and low energy measurements for constraining Higgs CP violation has been explored in Refs. [7–10].

Alternatively, it is also possible to extend the fermion sector of the SM while keeping the scalar sector minimal. The simplest case is to introduce a chiral fourth generation or mirror family, but they are strongly disfavored after the discovery of the Higgs boson, since they would lead to a large enhancement in the Higgs production rate. The next simplest extension is to introduce vectorlike quarks (VLQs). Vectorlike fermions are defined as having the same gauge quantum numbers for both left- and right-handed fermion pairs, and thus they do not generate chiral anomalies and their effects decouple in Higgs physics. They are the ingredients of beyond the SM frameworks like the little Higgs [11] or composite Higgs models [12, 13], and theories of extra dimensions [14–16] or extended supersymmetry [17, 18]. VLQs have also been discussed recently in light of modified Higgs couplings such as that to two photons [19, 20].<sup>1</sup> The current LHC lower limit on the masses of VLQs from direct searches is around 800 GeV [24] regardless of the decay modes. The indirect effects of VLQs in electroweak precision measurements and flavor physics have also been extensively

---

<sup>1</sup> There are also recent studies which extend both scalar and fermion sectors of the SM [21–23].

explored in the literature [25–29].

In this work, we consider the CP violating aspects of the VLQ models, which have been less studied. Our goal is to examine their impact on the CP nature and interactions of the Higgs boson, as well as the low energy constraints[30]. For simplicity, we focus on the simple cases where VLQs are in a single representation of  $SU(3)_c \times SU(2)_L \times U(1)_Y$ . We consider only fermion representations that can have new Yukawa couplings with the SM quarks and Higgs doublet. These new Yukawa couplings could provide a new source of CP violation at the weak scale. Under these assumptions, we find that only the case where the VLQ lies in the  $(3, 2, 1/3)$  representation can generate significant CP violation in Higgs physics.

We study CP violating phenomenology in the doublet VLQ model using an effective theory language where the heavy VLQs have been integrated out. Then the CP violating effects manifest themselves through a new right-handed charged-current interaction mediated by the  $W$ -boson. We clarify the source of CP violation in this model in Section II. In Section III, we calculate the loop induced CP violating Higgs interactions with gauge bosons. Interestingly, we find that CP violation only exists in the  $hWW$  coupling, but not in the  $hZZ$ [31],  $h\gamma\gamma$ , or  $hZ\gamma$ [32] ones. In Section IV, we explore the current constraints on this coupling from low energy measurements, including EDMs and  $B$  physics, and comment on the future prospects.

## II. CP VIOLATION FROM VECTORLIKE QUARKS

The vectorlike quark representations that allow new Yukawa couplings with SM quarks are summarized in Table I<sup>2</sup>.

The key point we want to make is that only the doublet  $(T, B)$  model can offer non-zero (unsuppressed) CP violation for the Higgs boson, through the Yukawa coupling to third generation quarks<sup>3</sup>. To see this, we write the Yukawa sector of this model,

$$\mathcal{L}_Y = y_t \bar{Q}_{3L} \tilde{H} t_R + y_b \bar{Q}_{3L} H b_R + M \bar{Q}'_L Q'_R + M' \bar{Q}_{3L} Q'_R + \lambda_t \bar{Q}'_L \tilde{H} t_R + \lambda_b \bar{Q}'_L H b_R + \text{h.c.}, \quad (1)$$

where  $H = (\phi^+, \phi_0)^T$  is the SM Higgs doublet,  $\tilde{H} = i\sigma_2 H^*$ ,  $Q_{3L}^T = (t_L, b_L)$  is the third generation left-handed quark doublet and  $Q_{L,R}^T = (T, B)_{L,R}$  are the vectorlike quark doublets.

<sup>2</sup> We find that introducing any number of singlet  $T_{L,R}$  and/or  $B_{L,R}$  fields does not give rise to new CP violating phases since any potential new phases can always be rotated away by a field redefinition.

<sup>3</sup> We assume only one representation of VLQs is present.

VLQ models	Representation	CP violation
$T_{L,R}$	$(3, 1, 4/3)$	no
$B_{L,R}$	$(3, 1, -2/3)$	no
$(T, B)_{L,R}$	$(3, 2, 1/3)$	yes
$(X, T)_{L,R}$	$(3, 2, 7/3)$	no
$(B, Y)_{L,R}$	$(3, 2, -5/3)$	no
$(X, T, B)_{L,R}$	$(3, 3, 4/3)$	no
$(T, B, Y)_{L,R}$	$(3, 3, -2/3)$	no

TABLE I. Models of vectorlike quarks and their representations under  $SU(3)_c \times SU(2)_L \times U(1)_Y$ , together with the possibilities of introducing new physical CP violating phases.

In general, the SM gauge invariance permits us to generalize the fields above,  $(Q_{3L}, t_R, b_R)$ , to linear combinations of all three generations. In our study, we assume the fields of Eq. (1) are dominantly composed of third generation fermions, because they have the largest Yukawa couplings and thus have the strongest impact on CP violation in Higgs physics, which is the motivation of this work. To be concrete, we can take advantage of the hierarchical structure of the CKM matrix, and define Eq. (1) in the basis where the SM  $3 \times 3$  blocks of the up- and down-type Yukawa matrices are close to diagonal up to CKM-like rotations<sup>4</sup>. This helps to suppress the mixing between heavy VLQs and the first two generation quarks and minimize the low energy flavor changing effects in the spirit of next-to-minimal flavor violation [33].

From now on, we will focus on the mixing between VLQs and the third generation quarks. Since  $Q_{3L}$  and  $Q'_L$  have the same quantum numbers, one can always redefine fields and set the parameter  $M' = 0$ . After electroweak symmetry breaking, the quark mass matrices take the form,

$$\mathcal{L}_m = (\bar{t}_L, \bar{T}_L) \begin{pmatrix} \frac{y_t v}{\sqrt{2}} & 0 \\ \frac{\lambda_t v}{\sqrt{2}} & M \end{pmatrix} \begin{pmatrix} t_R \\ T_R \end{pmatrix} + (\bar{b}_L, \bar{B}_L) \begin{pmatrix} \frac{y_b v}{\sqrt{2}} & 0 \\ \frac{\lambda_b v}{\sqrt{2}} & M \end{pmatrix} \begin{pmatrix} b_R \\ B_R \end{pmatrix}. \quad (2)$$

In general the parameters are all complex, and one can remove unphysical phases by redefining the phases of the fields. Under the gauge invariant transformations,  $Q'_R \rightarrow Q'_R e^{i\alpha}$ ,

<sup>4</sup> Alternatively, we could work in the basis where the  $3 \times 3$  block of down quark Yukawa couplings is already diagonal. With this assumption, the down quark sector is free from new contributions to flavor violating processes.

$Q'_L \rightarrow Q'_L e^{i\beta}$ ,  $Q_{3L} \rightarrow Q_{3L} e^{i\gamma}$ ,  $t_R \rightarrow t_R e^{i\delta}$ ,  $b_R \rightarrow b_R e^{i\sigma}$ , the parameters change to

$$\begin{aligned} y_t &\rightarrow y_t e^{i(\delta-\gamma)}, & \lambda_t &\rightarrow \lambda_t e^{i(\delta-\beta)}, \\ y_b &\rightarrow y_b e^{i(\sigma-\gamma)}, & \lambda_b &\rightarrow \lambda_b e^{i(\sigma-\beta)}, \\ M &\rightarrow M e^{i(\alpha-\beta)}. \end{aligned} \quad (3)$$

Clearly, what is invariant is the combination of phases of the parameters  $\arg(y_b) + \arg(\lambda_t) - \arg(y_t) - \arg(\lambda_b)$ , or the quantity,

$$\text{Im}(y_b \lambda_t y_t^* \lambda_b^*) \equiv |y_t y_b \lambda_b \lambda_t| e^{i\theta}. \quad (4)$$

This is the only new source of CP violation in this model that can enter into physical processes. It is convenient to use the above rephasing freedom to rotate the phase  $\theta$  into  $\lambda_t$  and make the other parameters real. In this case, from the quark mass terms,  $y_q(v+h)\bar{q}q/\sqrt{2}$ , we can first assign the Higgs boson to be CP even. Then any coupling between  $h$  and CP odd operators induced by Eq. (4) indicates CP is violated in the Higgs sector.

We diagonalize the mass matrices in Eq. (2), and obtain the mass eigenstates

$$\begin{aligned} \hat{t}_R &= \cos \theta_R^t t_R + \sin \theta_R^t e^{-i\theta} T_R, \\ \hat{b}_R &= \cos \theta_R^b b_R + \sin \theta_R^b B_R, \end{aligned} \quad (5)$$

where  $\hat{T}_R, \hat{B}_R$  are orthogonal to  $\hat{t}_R, \hat{b}_R$ , respectively. There are similar mixings among the left-handed fields, parametrized by angles  $\theta_L^t$  and  $\theta_L^b$ . The mixing angles among the right-handed quarks satisfy,

$$\tan 2\theta_R^i = \frac{\sqrt{2}M\lambda_i v}{M^2 - (\lambda_i^2 + y_i^2)v^2/2} \simeq \frac{\sqrt{2}\lambda_i v}{M}, \quad (i = t, b), \quad (6)$$

and the last step keeps only the leading term in the  $v/M$  expansion. The angle  $\theta_R^b$  denotes the mixing between the  $SU(2)_L$  singlet  $b_R$  and doublet  $B_R$ , and is constrained by electroweak precision measurements such as  $Z \rightarrow b\bar{b}$  [25, 34, 35]. The mixings among left-handed quark fields only appear at order  $(v/M)^2$  and are much smaller [25, 26].

The lower bound on the VLQ mass scale is around 800 GeV from direct searches at the LHC [24], which suggests that we can integrate them out when studying Higgs physics. Since  $T_R, B_R$  lie in an  $SU(2)_L$  doublet, integrating out the heavy vectorlike quarks yields an anomalous  $Wtb$  interaction,

$$\mathcal{L}_{eff} = a_R \left( \frac{g}{\sqrt{2}} \right) \bar{\hat{t}}_R \gamma^\mu \hat{b}_R W_\mu^+, \quad (7)$$

where

$$a_R = \sin \theta_R^t \sin \theta_R^b e^{i\theta} \simeq \frac{|\lambda_b \lambda_t| v^2}{2M^2} e^{i\theta}. \quad (8)$$

As discussed above, in this model CP violation must appear in physical processes through the combination of couplings,  $\text{Im}(y_b \lambda_t y_t^* \lambda_b^*)$ . The new right-handed  $Wtb$  coupling  $a_R$  obtained here is proportional to  $\lambda_t \lambda_b^*$ . Therefore, a physical process that makes the CP violation manifest should involve both left- and right-handed currents in order to allow mass (Yukawa coupling  $y_t, y_b$ ) insertions. We write the most general renormalizable  $Wtb$  coupling as

$$\mathcal{L}_{eff} = \frac{g}{\sqrt{2}} \bar{t} (a_L P_L + a_R P_R) b W_\mu^+ + h.c.. \quad (9)$$

We neglect the hat symbol for mass eigenstates hereafter. In the SM,  $a_L = V_{tb} \simeq 1$  and  $a_R = 0$ . For the vectorlike quark doublet model we consider,  $a_R$  is given by Eq. (8), and the deviation of  $a_L$  from 1 occurs only at higher order in  $v/M$ .

Following a similar reasoning, we have also examined other representations of VLQs. Interestingly, none of them can offer an irreducible CP violating phase such as that in Eq. (4), *i.e.*, under the same assumptions, the Higgs boson is essentially CP even in those models. This observation places the VLQ doublet  $(T, B)$  model in a unique place in the perspective of CP violation. In the coming sections, we will explore the  $(T, B)$  model as a theory of Higgs CP violation, and study in detail its predictions in phenomenology and the constraints on the parameters of the model.

### III. CP VIOLATION IN HIGGS BOSON INTERACTIONS

The Yukawa interactions between vectorlike and SM quarks introduce a new source of CP violation. One of the consequences is that the Higgs boson will obtain CP violating interactions with the other SM particles. As discussed in Eq. (4), in the model with a single VLQ doublet,  $(T, B)$ , the physical CP violating phase has to appear via the combination of parameters,  $\text{Im}(y_b \lambda_t y_t^* \lambda_b^*)$ . This means that the diagram giving CP violating interactions to the Higgs boson must involve both top and bottom quarks. As a result, the leading CP violation in this model resides only in the  $hW_{\mu\nu}^+ \tilde{W}^{-\mu\nu}$  operator, generated at loop level as shown in the left diagram of Fig. 1. At this order, CP violating tree level Higgs-quark or

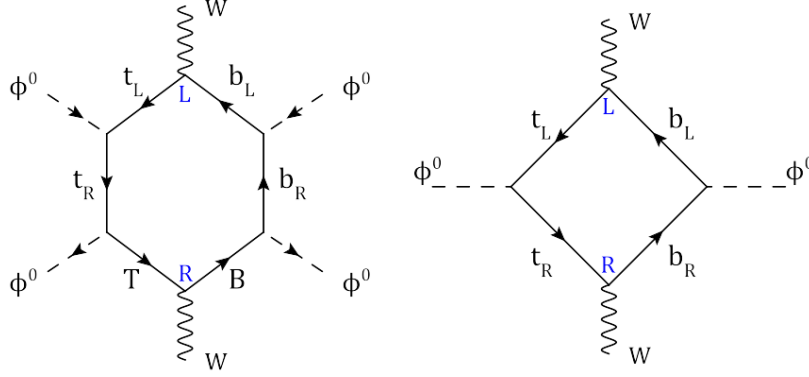


FIG. 1. Feynman diagrams generating CP violating Higgs couplings. The label “L (R)” means a left- (right-) handed current interaction with the  $W$ -boson. The left diagram is in the full theory, and the right one is in the effective theory when the vectorlike quarks are integrated out. The right-handed current  $Wtb$  vertex is derived in Eq. (9). For the  $hWW$  coupling, one of the  $\phi^0$  fields is replaced by the electroweak vev, and the other replaced by  $h$ .

loop level Higgs- $Z$ -boson and Higgs-photon interactions are absent. The direct probes of CP violating  $hWW$  interactions at the LHC have been discussed in the  $h \rightarrow WW$  decay, the  $hW$  associated production channel and the  $WW$  fusion channel [36, 37].

In the heavy fermion limit, the gauge invariant operator generating the Higgs-gauge boson CP violation starts from dimension 8 in this model,

$$\mathcal{L}_8 = \frac{C_8}{\Lambda^4} [\epsilon_{ij} H^i (\sigma^a)^j_k H^k W_{\mu\nu}^a] \left[ \epsilon_{mn} H^m (\sigma^b)^n_l H^l \tilde{W}^{b\mu\nu} \right]^* , \quad (10)$$

$\sigma^a$  are the Pauli matrices,  $\tilde{W}_{\mu\nu} = \frac{1}{2} \epsilon_{\mu\nu\alpha\beta} W^{\alpha\beta}$  and  $i, j, k, l, m, n = 1, 2$  are  $SU(2)_L$  indices. After electroweak symmetry breaking,  $H^1 \equiv \phi^+ = 0$  and  $H^2 \equiv \phi^0 = (v + h)/\sqrt{2}$  in the unitary gauge. This projects out the CP violating  $hW_{\mu\nu}^+ \tilde{W}^{-\mu\nu}$  interaction

$$\mathcal{L}_8 \rightarrow \frac{2C_8 v^3}{\Lambda^4} h W_{\mu\nu}^a \tilde{W}_{\mu\nu}^{a*} \equiv a_3^W \frac{h}{v} W_{\mu\nu}^a \tilde{W}_{\mu\nu}^{a*} . \quad (11)$$

In the last step, we define the coefficient  $a_3^W$  in the same notation as Eq. (1.15) in the Higgs Working Group Snowmass report [38].

In reality, because the top quark mass is comparable to the center-of-mass energy  $\sqrt{s}$  in the Higgs production and decay processes, the coefficient  $a_3^W$  becomes a form factor. We first calculate the form factor for CP violating  $W(q_1)h(p)$  associated production [39, 40] via an off-shell  $W^*(q_2)$ . In this case, the momenta satisfy  $q_1^2 = M_W^2$ ,  $p^2 = m_h^2$  and  $s = q_2^2 \geq (m_h + M_W)^2$ .

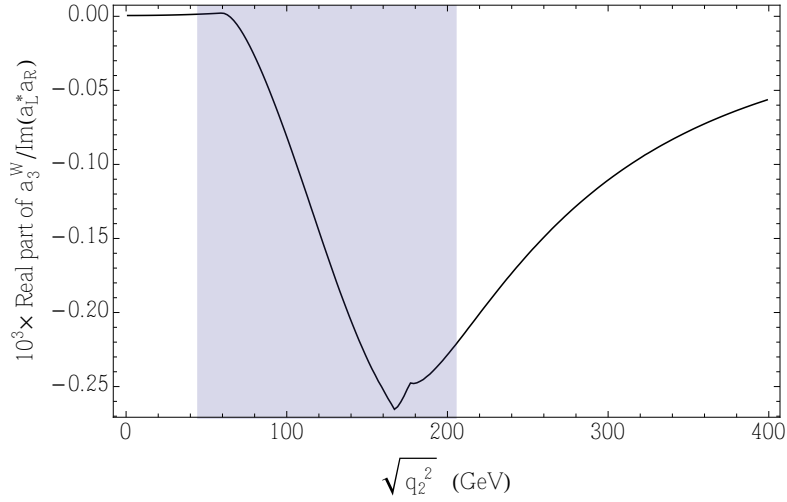


FIG. 2. Real part of the form factor  $a_3^W$  as a function of  $\sqrt{q_2^2}$  in units of  $10^{-3} \times \text{Im}(a_L^* a_R)$ . For  $Wh$  associated production, the kinematics require  $\sqrt{q_2^2} > m_h + M_W$ , *i.e.*, the white region to the right of the shaded region. For  $h \rightarrow WW^*$  associated production, the kinematics require  $0 < \sqrt{q_2^2} < m_h - M_W$ , *i.e.*, the white region to the left of the shaded region.

The leading contribution to the form factor  $a_3^W$  can be conveniently calculated in the effective theory when the vectorlike quarks are integrated out, as shown on the righthand side of Fig. 1. We find

$$a_3^W(\sqrt{q_2^2}) \simeq \frac{\sqrt{2}N_c G_F m_t m_b}{4\pi^2} \text{Im}(a_L^* a_R) \int_0^1 dx \int_0^{1-x} dy (1-x-y) \left[ \frac{1}{\Delta_t} - \frac{1}{\Delta_b} \right], \quad (12)$$

where the denominators are

$$\begin{aligned} \Delta_t &= (x+y)z_t^2 - xyz_h^2 + (x+y-1)(xz_1^2 + yz_2^2 - z_b^2), \\ \Delta_b &= (x+y)z_b^2 - xyz_h^2 + (x+y-1)(xz_1^2 + yz_2^2 - z_t^2), \end{aligned} \quad (13)$$

and  $q_i^2$  are the off-shell momenta of the  $W$  gauge bosons,  $z_a = m_a/M_W$ , ( $a = t, h, b$ ),  $z_1^2 = q_1^2/M_W^2 = 1$ , and  $z_2^2 = q_2^2/M_W^2 = s/M_W^2$ . The  $1/\Delta_{t,b}$  terms correspond to the diagrams where the Higgs field is attached to the top (bottom) quark propagators. There is a minus sign between the two pieces in the integrand of the Feynman parameter integral. From the analysis of [37], only the real part of the form factor  $a_3^W$  contributes to the final CP violation observable, *i.e.*, a phase shift in azimuthal angle. In Fig. 2, we plot the real part of  $a_3^W$  as a function of  $\sqrt{q_2^2}$ . For  $Wh$  associated production, the kinematics require  $\sqrt{q_2^2} > m_h + M_W$ , *i.e.*, the physical region is the white region to the right of the shaded region in the plot.

We next examine the form factor in the decay process  $h(p) \rightarrow W(q_1)W^*(q_2)$ . In this case, the momenta satisfy  $p^2 = m_h^2$ ,  $q_1^2 = M_W^2$ ,  $0 \leq q_2^2 \leq (m_h - M_W)^2$ . The integral of the  $1/\Delta_t$  term is real. On the other hand, the integral of the  $1/\Delta_b$  term has an imaginary (absorptive) part, which is due to a pole in  $y$  corresponding to the on-shell cut of the  $b\bar{b}$  propagators. Numerically, we find the integral over  $1/\Delta_t$  and dispersive part of the  $1/\Delta_b$  integral almost cancel each other. The integral is dominated by the absorptive part of the  $1/\Delta_b$  integral, which we find to be of order 1 for all values of  $q_2^2$ . Physically, it indicates that the CP violating effect in the  $h \rightarrow WW^*$  decay is dominated by processes where the Higgs boson first decays to  $b\bar{b}$  and then the  $b\bar{b}$  re-scatter into  $WW^*$ <sup>5</sup>.

The coefficient  $a_3^W$  calculated above is proportional to the quantity  $\text{Im}(a_L^* a_R)$  and is of the order  $(v/M)^2$ . There is another contribution obtained by changing the right-handed current to a left-handed one in the heavy quark vertex (left diagram of Fig. 1), and we have checked that this contribution is  $\mathcal{O}(v/M)^4$  and is subdominant.

Using the central values of masses and constants from the PDG [41], we find in both processes the coefficient for the CP violating  $hWW$  interaction is

$$a_3^W \simeq 10^{-3} \times \text{Im}(a_L^* a_R). \quad (14)$$

The first factor contains the usual loop factor and the bottom quark Yukawa coupling. The CP violating parameter  $\text{Im}(a_L^* a_R)$  depends on the model parameters  $\lambda_b, \lambda_t$ . The goal of the next section is to explore the current and future experimental constraints (sensitivities) to  $\text{Im}(a_L^* a_R)$ .

#### IV. CONSTRAINTS

In this section, we explore phenomenological constraints on the parameter  $\text{Im}(a_L^* a_R)$  relevant for the CP violating  $hWW$  coupling. We find the most relevant limits come from the electric dipole moments and the rate and CP asymmetry of the rare  $B$  decay  $b \rightarrow s\gamma$ .

---

<sup>5</sup> In general a cut is not necessary for CP violation to occur because the final state  $W^+W^-$  is already an eigenstate under CP. The cancelation between the  $1/\Delta_t$  and dispersive part of the  $1/\Delta_b$  integrals seems accidental.

## A. Electric Dipole Moments

Electric dipole moments are sensitive probes of new sources of CP violation. We first study the constraint from the electron EDM. The interactions Eq. (9) can contribute to the electron EDM through the two-loop Barr-Zee type diagrams as shown in Fig. 3. This contribution has been calculated analytically in Ref. [42],

$$\begin{aligned} \frac{d_e}{e} = & -\frac{\alpha^2}{8\pi^2 \sin^4 \theta_W M_W} z_e z_t z_b \text{Im}(a_L^* a_R) \\ & \times \frac{Q_b}{2} \int_0^1 dx_1 \int_0^{1-x_1} dx_2 \left[ \frac{x(x-1)}{(g_b - x(1-x))^2} \log \frac{g_b}{x(1-x)} - \frac{1}{g_b - x(1-x)} \right] - (b \leftrightarrow t), \end{aligned} \quad (15)$$

where  $x = x_1 + x_2$ ,  $z_a = m_a/M_W$ , ( $a = e, t, b$ ), and  $g_t = x(z_t^2 - z_b^2) + z_b^2$ ,  $g_b = x(z_b^2 - z_t^2) + z_t^2$ . Here  $d_e$  is the coefficient of the effective EDM operator,

$$\mathcal{L}_{eff} \supset d_e \left( \frac{-i}{2} \right) \bar{e} \sigma_{\mu\nu} \gamma_5 e F^{\mu\nu}. \quad (16)$$

Numerically, we find,

$$d_e \simeq -1.58 \times 10^{-27} \text{Im}(a_L^* a_R) e \cdot \text{cm}. \quad (17)$$

The current experimental upper limit on the electron EDM is  $|d_e| < 8.7 \times 10^{-29} e \cdot \text{cm}$  at 90% CL from the ACME experiment in 2013 [43]. This translates into the upper bound,

$$|\text{Im}(a_R)| < 0.055. \quad (18)$$

It turns out that the electron EDM constraint is weaker than the one from  $B$  physics, as will be discussed in the next subsection, although the EDM constraint will become relevant if the current ACME limit is improved by only a factor of a few. In Fig. 5, the horizontal magenta dotted line shows the future exclusion if the limit reaches 10 times the ACME-2013 limit.

Next, we consider the EDMs of the neutron, the proton and the mercury atom. These constraints usually involve large hadronic and nuclear physics uncertainties. However, given the future prospects of these experiments, they could become relevant. There are several contributions to these observables. The first includes light quark EDMs, from a similar diagram as Fig. 3, with the replacement  $(e, \nu) \rightarrow (u, d)$  or  $(d, u)$ . At  $\mu = 1 \text{ GeV}$ ,

$$d_u(\mu) \simeq -2.3 \times 10^{-26} \eta_1 \text{Im}(a_L^* a_R) e \cdot \text{cm}, \quad (19)$$

$$d_d(\mu) \simeq -4.6 \times 10^{-26} \eta_1 \text{Im}(a_L^* a_R) e \cdot \text{cm}. \quad (20)$$

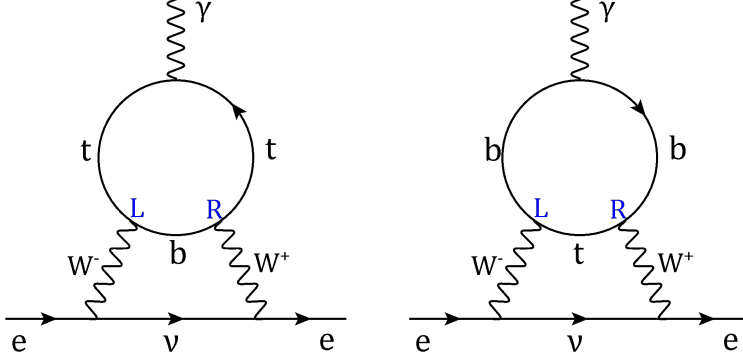


FIG. 3. Barr-Zee diagrams that contribute to electron EDM. The crossed diagrams with  $L \leftrightarrow R$  are not shown.

Here the renormalization group (RG) running effect from the  $M_W$  scale down to the GeV scale is taken into account,

$$\eta_1 = \left[ \frac{\alpha_s(M_W)}{\alpha_s(m_b)} \right]^{\frac{16}{23}} \left[ \frac{\alpha_s(m_b)}{\alpha_s(m_c)} \right]^{\frac{16}{25}} \left[ \frac{\alpha_s(m_c)}{\alpha_s(1 \text{ GeV})} \right]^{\frac{16}{27}} \simeq 0.417. \quad (21)$$

Hereafter we have used the NLO values of  $\alpha_s$  at various scales in the following table.

$\alpha_s(M_W)$	$\alpha_s(m_b)$	$\alpha_s(m_c)$	$\alpha_s(1 \text{ GeV})$
0.120808	0.218894	0.382156	0.455862

The contribution of Eq. (19), (20) to the neutron EDM,  $d_n \sim -0.35d_u(\mu) + 1.4d_d(\mu)$ , is too small to yield a competitive constraint on  $\text{Im}(a_L^* a_R)$  in view of the current limit  $|d_n| < 2.9 \times 10^{-26} e \cdot \text{cm}$ .

There is no light quark chromo-EDM at one loop level in the VLQ model. Instead, there is a contribution to the chromo-EDM of the bottom quark, shown in Fig. 4<sup>6</sup>. The bottom quark chromo-EDM can contribute to the EDMs via matching to the three-gluon Weinberg operator at a low scale. The effective Lagrangian for the two operators takes the form [44],

$$\mathcal{L}_{eff} \supset i \frac{\tilde{\delta}_b}{\Lambda^2} g_s m_b \bar{b} \sigma_{\mu\nu} \gamma_5 T^a b G^{a\mu\nu} + \frac{C_{\tilde{G}}}{2\Lambda^2} g_s f^{abc} \epsilon^{\mu\nu\rho\sigma} G_{\mu\lambda}^a G_\nu^b G_{\rho\sigma}^c. \quad (22)$$

The calculation of the coefficient of the chromo-EDM operator is similar to that in the left-right symmetric model [45]. At the weak scale,

$$\frac{\tilde{\delta}_b(M_W)}{\Lambda^2} = -\frac{\sqrt{2}G_F}{8\pi^2} \frac{m_t}{m_b} \text{Im}(a_L^* a_R) f(z_t), \quad (23)$$

<sup>6</sup> Unlike Ref. [42], we find that diagrams similar to Fig. 3 but with photon lines replaced by gluon ones and leptons replaced by light quarks vanish and do not give rise to Chromo-EDMs.

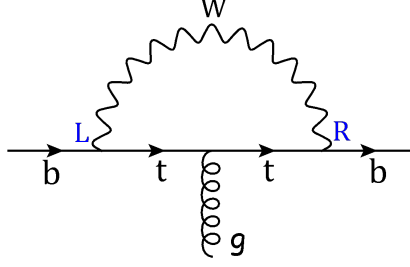


FIG. 4. One-loop contribution to the bottom quark chromo-EDM.

where  $f(z_t) = [1 - \frac{3}{4}z_t^2 - \frac{1}{4}z_t^6 + \frac{3}{2}z_t^2 \log z_t^2] / (1 - z_t^2)^3 \simeq 0.35$ . Interestingly, there is an enhancement factor  $(m_t/m_b)$  [46]. At the scale  $m_b$ , the matching condition is  $C_{\tilde{G}}(m_b) = \frac{1}{12\pi}\alpha_s(m_b)\tilde{\delta}_b(m_b)$  [7]. Taking into account the RG running, the coefficient  $C_{\tilde{G}}$  at  $\mu = 1 \text{ GeV}$  is,

$$\frac{C_{\tilde{G}}(\mu)}{\Lambda^2} = \frac{\alpha_s(m_b)}{12\pi} \left[ \frac{\alpha_s(M_W)}{\alpha_s(m_b)} \right]^{\frac{14}{23}} \left[ \frac{\alpha_s(m_b)}{\alpha_s(m_c)} \right]^{\frac{29}{25}} \left[ \frac{\alpha_s(m_c)}{\alpha_s(1 \text{ GeV})} \right] \frac{\tilde{\delta}_b(M_W)}{\Lambda^2} \simeq -\frac{4.5 \times 10^{-9} \text{Im}(a_L^* a_R)}{\text{GeV}^2} \quad (24)$$

The final contribution to the neutron EDM is dominated by the Weinberg operator [7, 44],

$$d_n \simeq (2 \times 10^{-20} e \cdot \text{cm}) \left( \frac{v^2}{\Lambda^2} \right) C_{\tilde{G}}(\mu) \simeq -5.5 \times 10^{-24} \text{Im}(a_L^* a_R) e \cdot \text{cm}, \quad (25)$$

where we have used the hadronic matrix element given in Ref. [7]. The current limit on the neutron EDM,  $|d_n| < 2.9 \times 10^{-26} e \cdot \text{cm}$  at 95% CL, translates into the upper bound,

$$|\text{Im}(a_L^* a_R)| < 0.5 \times 10^{-2}. \quad (26)$$

Because the three-gluon operator is an isospin singlet, the proton EDM in this model is equal to the neutron EDM. A possible future experiment measuring the proton EDM is expected to give a strong constraint [47, 48].

The EDM of mercury  $^{199}\text{Hg}$  is also sensitive to the three-gluon operator, which contributes through the Schiff moment [7, 44],

$$d_{\text{Hg}} = \kappa_S \frac{2g_A m_N}{F_\pi} \left( a_0 \gamma_{(0)}^{\tilde{G}} + a_1 \gamma_{(1)}^{\tilde{G}} \right) \left( \frac{v^2}{\Lambda^2} \right) C_{\tilde{G}} \simeq 3.9 \times 10^{-27} \text{Im}(a_L^* a_R) e \cdot \text{cm}, \quad (27)$$

where we have used the conventions and values of parameters given in Ref. [7]. The current limit on the mercury EDM,  $|d_{\text{Hg}}| < 3.1 \times 10^{-29} e \cdot \text{cm}$ , translates into the upper bound,

$$|\text{Im}(a_L^* a_R)| < 0.8 \times 10^{-2}. \quad (28)$$

## B. B physics

There are strong constraints on the parameter  $\text{Im}(a_L^* a_R)$  from the  $b \rightarrow s\gamma$  channel, both from the total rate and the CP asymmetry. The effective Lagrangian relevant for this process takes the form,

$$\mathcal{L}_{eff}^{(b \rightarrow s\gamma)} = c_7 \frac{em_b}{16\pi^2} \bar{s}_L \sigma^{\mu\nu} b_R F_{\mu\nu} + c_8 \frac{g_s m_b}{16\pi^2} \bar{s}_L \sigma^{\mu\nu} T^a b_R G_{\mu\nu}^a. \quad (29)$$

The contribution of new right-handed current interaction to the Wilson coefficients at the scale  $M_W$  are [49],

$$\begin{aligned} \Delta c_7(M_W) &= a_R \frac{m_t}{m_b} f_7(m_t^2/M_W^2), \\ \Delta c_8(M_W) &= a_R \frac{m_t}{m_b} f_8(m_t^2/M_W^2), \end{aligned} \quad (30)$$

where the form factors are,

$$\begin{aligned} f_7(x) &= \frac{-3x^2 + 2x}{2(x-1)^3} \log x + \frac{-5x^2 + 31x - 20}{12(x-1)^2}, \\ f_8(x) &= \frac{3x}{2(x-1)^3} \log x - \frac{x^2 + x + 4}{4(x-1)^2}. \end{aligned} \quad (31)$$

When we take into account the 1-loop RG running corrections from  $M_W$  to  $\mu = m_b$ , the effective coefficients are [50],

$$\begin{aligned} c_7(\mu) &= a_L c_7^{\text{SM}}(\mu) + \eta_b^{16/23} \Delta c_7(M_W) + \frac{8}{3} (\eta_b^{14/23} - \eta_b^{16/23}) \Delta c_8(M_W), \\ c_8(\mu) &= a_L c_8^{\text{SM}}(\mu) + \eta_b^{14/23} \Delta c_8(M_W), \end{aligned} \quad (32)$$

with  $c_7^{\text{SM}}(\mu) = -0.31$ ,  $c_8^{\text{SM}}(\mu) = -0.15$  and  $\eta_b = \alpha_s(M_W)/\alpha_s(m_b) \simeq 0.55$ .

The  $B \rightarrow X_s \gamma$  decay rate in the VLQ model is then given by

$$\mathcal{B}(B \rightarrow X_s \gamma) = \mathcal{B}(B \rightarrow X_s \gamma)_{\text{SM}} \left| \frac{c_7}{c_7^{\text{SM}}} \right|^2. \quad (33)$$

The SM prediction has a central value  $\mathcal{B}(B \rightarrow X_s \gamma)_{\text{SM}} = 3.15 \times 10^{-4}$ . The world average of the measurements is  $\mathcal{B}(B \rightarrow X_s \gamma) = (3.55 \pm 0.24 \pm 0.09) \times 10^{-4}$  [51].

In order to present this result as a limit, we note the fact that in the VLQ model the contribution to  $a_R$  dominates over the deviation  $a_L - 1$ . Using results from the EDM discussions that  $\text{Im}(a_L^* a_R)$  is already constrained to be less than  $\sim 10^{-2}$ , we conclude that

$$\text{Im}(a_L^* a_R) \simeq \text{Im}(a_R). \quad (34)$$

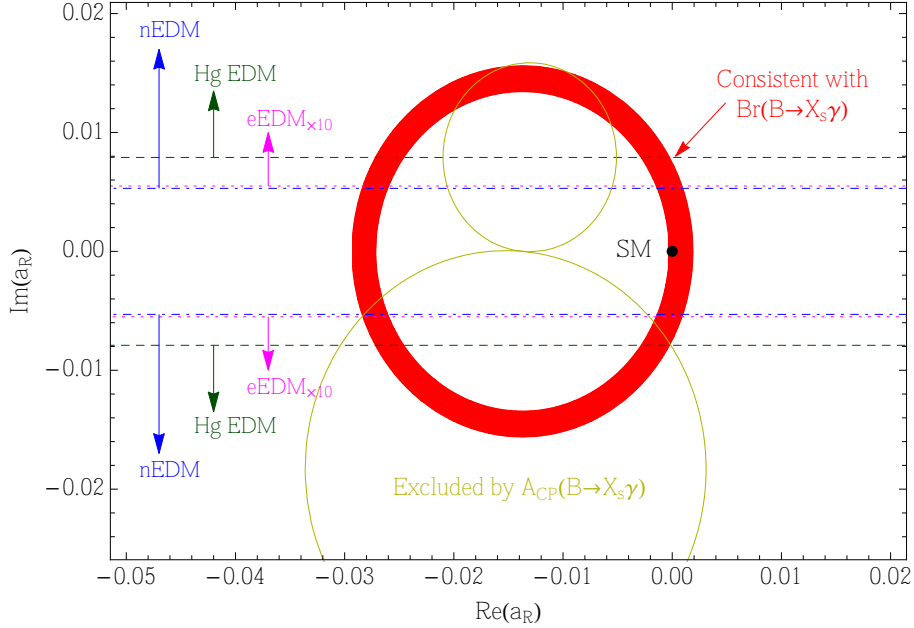


FIG. 5. Constraints on the  $\text{Re}(a_R)$  and  $\text{Im}(a_R)$  parameter space from EDMs and the  $B \rightarrow X_s \gamma$  decay. The red shaded region is consistent with the branching ratio  $\mathcal{B}(B \rightarrow X_s \gamma)$ . The regions inside the solid yellow circles are excluded by the direct CP asymmetry,  $A_{CP}$ , in  $B \rightarrow X_s \gamma$  decay. The EDM constraints are shown by the blue dot-dashed lines (current neutron EDM, central value), green dashed lines (current mercury EDM) and magenta dotted lines (future electron EDM with 10 times better limit than the current one from ACME). The exclusion regions are in the direction of arrows. The neutron and mercury EDM typically involve large nuclear/hadronic uncertainties, and here the lines only show the central value of their bounds.

In this case, the constraint from the  $B \rightarrow X_s \gamma$  decay rate measurement is presented in the parameter space of  $\text{Re}(a_R)$  versus  $\text{Im}(a_R)$ , as shown by the red shaded region in Fig. 5.

The direct CP asymmetry in  $B \rightarrow X_s \gamma$  decay rate is [52]

$$A_{CP} = \alpha_s(m_b) \left\{ \frac{40}{81} \text{Im} \left( \frac{c_2}{c_7} \right) - \frac{4}{9} \text{Im} \left( \frac{c_8}{c_7} \right) - \frac{40 \Lambda_c}{9 m_b} \text{Im} \left[ (1 + \epsilon_s) \frac{c_2}{c_7} \right] \right\}, \quad (35)$$

where  $c_2 = 1.11$ ,  $\epsilon_s = -0.007 + 0.018i$ ,  $\Lambda_c = 0.38 \text{ GeV}$ , and  $\alpha_s(m_b) = \alpha_s(M_W)/\eta = 0.21$ . The most stringent experimental measurement is from BaBar,  $A_{CP} = (1.7 \pm 1.9 \pm 1.0)\%$  [53]. Again, we show this as a constraint in the  $\text{Re}(a_R)$  versus  $\text{Im}(a_R)$  plane in Fig. 5. The regions inside the yellow circles are excluded.

Summarizing the EDM and the  $B$  physics constraints, we conclude that in the doublet

VLQ model it is still possible to have  $\text{Im}(a_R)$  as large as order 0.01. From Eq. (14), this implies the CP violating  $hWW$  coupling  $a_3^W$  is currently constrained to be at most  $10^{-5}$ . The next generation EDM search is expected to further narrow down the allowed window of  $\text{Im}(a_R)$ . In the case of discovery, this would trigger an exciting interplay between the studies of CP violation in a future  $B$  factory and a future Higgs factory.

## V. CONCLUSION

In this work, we have studied the possibility of introducing CP violating interactions to the 125 GeV Higgs boson by extending the fermion sector of the SM with vectorlike quarks. We examined the simplest class of models where VLQs arise from a single representation under the SM gauge group. There are 7 possible representations where the VLQs have Yukawa interactions with the SM third generation quarks and Higgs doublets. The new complex Yukawa couplings could accommodate new sources of CP violation. Among them, we find that an irreducible CP phase shows up only for one representation of VLQ, which is a doublet under  $SU(2)_L$  and carries hypercharge 1/3. For the other representations all the phases can be rotated away and are unphysical.

We study the CP violating phenomenology in the doublet VLQ model. Since the VLQs are already constrained to be heavier than 800 GeV by the LHC, we integrate them out and study the effective theory, where CP violation manifests itself through a new right-handed charged current mediated by the SM  $W$ -boson. We have calculated the CP violating Higgs interactions with SM gauge bosons, generated at one loop level involving both top and bottom quarks. This corresponds to a dimension 8 operator in the heavy top/bottom quark limit. As a consequence, only the  $hWW$  coupling is CP violating, while the  $hZZ$ ,  $h\gamma\gamma$ ,  $hZ\gamma$  couplings are essentially CP conserving at this order. The strength of the CP violating  $hWW$  coupling is proportional to the quantity  $\text{Im}(a_L^* a_R)$ , where  $a_{L,R}$  are the coefficients of left- and right-handed current  $Wtb$  interactions, respectively. At low energy, we find the most relevant constraints on  $\text{Im}(a_L^* a_R)$  come from the electric dipole moments and the  $b \rightarrow s\gamma$  decay rate and CP asymmetry, which are in complimentary to each other. The current experimental constraints require  $\text{Im}(a_L^* a_R) \lesssim 0.01$ . They in turn imply that the coefficient of the CP violating  $hWW$  interaction,  $a_3^W$ , cannot be larger than of order  $10^{-5}$ , and, as we stress again, only in the  $hWW$  channel. We expect exciting interplays of various

experimental searches in the future to probe and distinguish new sources of CP violation near the electroweak scale.

## ACKNOWLEDGMENTS

We thank JiJi Fan, Enrico Lunghi, and Miha Nemevsek for useful discussions. The work of C.-Y. Chen and S. Dawson is supported by the U.S. Department of Energy under grant No. DE-AC02-98CH10886 and contract DE-AC02-76SF00515. This work of Y. Zhang is supported by the Gordon and Betty Moore Foundation through Grant #776 to the Caltech Moore Center for Theoretical Cosmology and Physics, and by the DOE Grant DE-FG02-92ER40701, and also by a DOE Early Career Award under Grant No. DE-SC0010255.

- 
- [1] Duarte Fontes, Jorge C. Romo, Joo P. Silva, and Rui Santos. Large pseudo-scalar components in the C2HDM. 2015.
  - [2] Duarte Fontes, Jorge C. Romo, Rui Santos, and Joo P. Silva. Undoubtable signs of CP-violation in Higgs decays at the LHC run 2. 2015.
  - [3] Duarte Fontes, Jorge C. Romo, Rui Santos, and Joo P. Silva. Large pseudoscalar Yukawa couplings in the complex 2HDM. *JHEP*, 06:060, 2015.
  - [4] L. Lavoura and Joao P. Silva. Fundamental CP violating quantities in a  $SU(2) \times U(1)$  model with many Higgs doublets. *Phys.Rev.*, D50:4619–4624, 1994.
  - [5] B. Grzadkowski, O.M. Ogreid, and P. Osland. Measuring CP violation in Two-Higgs-Doublet models in light of the LHC Higgs data. *JHEP*, 1411:084, 2014.
  - [6] John F. Gunion and Howard E. Haber. Conditions for CP-violation in the general two-Higgs-doublet model. *Phys.Rev.*, D72:095002, 2005.
  - [7] Satoru Inoue, Michael J. Ramsey-Musolf, and Yue Zhang. CP-violating phenomenology of flavor conserving two Higgs doublet models. *Phys.Rev.*, D89(11):115023, 2014.
  - [8] Chien-Yi Chen, S. Dawson, and Yue Zhang. Complementarity of LHC and EDMs for Exploring Higgs CP Violation. *JHEP*, 1506:056, 2015.
  - [9] Jing Shu and Yue Zhang. Impact of a CP Violating Higgs Sector: From LHC to Baryogenesis. *Phys.Rev.Lett.*, 111(9):091801, 2013.

- [10] Kingman Cheung, Jae Sik Lee, Eibun Senaha, and Po-Yan Tseng. Confronting Higgscision with Electric Dipole Moments. *JHEP*, 1406:149, 2014.
- [11] N. Arkani-Hamed, A. G. Cohen, E. Katz, A. E. Nelson, T. Gregoire, and Jay G. Wacker. The Minimal moose for a little Higgs. *JHEP*, 08:021, 2002.
- [12] David B. Kaplan, Howard Georgi, and Savas Dimopoulos. Composite Higgs Scalars. *Phys. Lett.*, B136:187, 1984.
- [13] Kaustubh Agashe, Roberto Contino, and Alex Pomarol. The Minimal composite Higgs model. *Nucl. Phys.*, B719:165–187, 2005.
- [14] Nima Arkani-Hamed, Savas Dimopoulos, and G. R. Dvali. The Hierarchy problem and new dimensions at a millimeter. *Phys. Lett.*, B429:263–272, 1998.
- [15] Lisa Randall and Raman Sundrum. A Large mass hierarchy from a small extra dimension. *Phys. Rev. Lett.*, 83:3370–3373, 1999.
- [16] Thomas Appelquist, Hsin-Chia Cheng, and Bogdan A. Dobrescu. Bounds on universal extra dimensions. *Phys. Rev.*, D64:035002, 2001.
- [17] Pierre Fayet.  $N = 2$  Extended Supersymmetric GUTs: Gauge Boson / Higgs Boson Unification, Mass Spectrum and Central Charges. *Nucl. Phys.*, B246:89, 1984.
- [18] F. del Aguila, M. Dugan, Benjamin Grinstein, Lawrence J. Hall, Graham G. Ross, and Peter C. West. Low-energy Models With Two Supersymmetries. *Nucl. Phys.*, B250:225, 1985.
- [19] M. B. Voloshin. CP Violation in Higgs Diphoton Decay in Models with Vectorlike Heavy Fermions. *Phys. Rev.*, D86:093016, 2012.
- [20] JiJi Fan and Matthew Reece. Probing Charged Matter Through Higgs Diphoton Decay, Gamma Ray Lines, and EDMs. *JHEP*, 1306:004, 2013.
- [21] David McKeen, Maxim Pospelov, and Adam Ritz. Modified Higgs branching ratios versus CP and lepton flavor violation. *Phys. Rev.*, D86:113004, 2012.
- [22] Wei Chao and Michael J. Ramsey-Musolf. Catalysis of Electroweak Baryogenesis via Fermionic Higgs Portal Dark Matter. 2015.
- [23] Shrihari Gopalakrishna, Tuhin Subhra Mukherjee, and Soumya Sadhukhan. CP-odd scalar with vector-like fermions at the LHC. 2015.
- [24] Georges Aad et al. Search for production of vector-like quark pairs and of four top quarks in the lepton-plus-jets final state in  $pp$  collisions at  $\sqrt{s} = 8$  TeV with the ATLAS detector. 2015.

- [25] S. Dawson and E. Furlan. A Higgs Conundrum with Vector Fermions. *Phys.Rev.*, D86:015021, 2012.
- [26] J.A. Aguilar-Saavedra, R. Benbrik, S. Heinemeyer, and M. Prez-Victoria. Handbook of vectorlike quarks: Mixing and single production. *Phys.Rev.*, D88(9):094010, 2013.
- [27] Svjetlana Fajfer, Admir Greljo, Jernej F. Kamenik, and Ivana Mustac. Light Higgs and Vector-like Quarks without Prejudice. *JHEP*, 1307:155, 2013.
- [28] Sebastian A.R. Ellis, Rohini M. Godbole, Shrihari Gopalakrishna, and James D. Wells. Survey of vector-like fermion extensions of the Standard Model and their phenomenological implications. *JHEP*, 1409:130, 2014.
- [29] Aielet Efrati, Adam Falkowski, and Yotam Soreq. Electroweak constraints on flavorful effective theories. *JHEP*, 07:018, 2015.
- [30] Vincenzo Cirigliano and Michael J. Ramsey-Musolf. Low Energy Probes of Physics Beyond the Standard Model. *Prog.Part.Nucl.Phys.*, 71:2–20, 2013.
- [31] Neil D. Christensen, Tao Han, and Yingchuan Li. Testing CP Violation in ZZH Interactions at the LHC. *Phys. Lett.*, B693:28–35, 2010.
- [32] S. Y. Choi, M. M. Muhlleitner, and P. M. Zerwas. Theoretical Basis of Higgs-Spin Analysis in  $H \rightarrow \gamma\gamma$  and  $Z\gamma$  Decays. *Phys. Lett.*, B718:1031–1035, 2013.
- [33] Kaustubh Agashe, Michele Papucci, Gilad Perez, and Dan Pirjol. Next to minimal flavor violation. 2005.
- [34] P. Bamert, C. P. Burgess, James M. Cline, David London, and E. Nardi.  $R(b)$  and new physics: A Comprehensive analysis. *Phys. Rev.*, D54:4275–4300, 1996.
- [35] Ayres Freitas. Higher-order electroweak corrections to the partial widths and branching ratios of the Z boson. *JHEP*, 04:070, 2014.
- [36] Sara Bolognesi, Yanyan Gao, Andrei V. Gritsan, Kirill Melnikov, Markus Schulze, Nhan V. Tran, and Andrew Whitbeck. On the spin and parity of a single-produced resonance at the LHC. *Phys. Rev.*, D86:095031, 2012.
- [37] Cdric Delaunay, Gilad Perez, Hiroshi de Sandes, and Witold Skiba. Higgs Up-Down CP Asymmetry at the LHC. *Phys. Rev.*, D89(3):035004, 2014.
- [38] Sally Dawson, Andrei Gritsan, Heather Logan, Jianming Qian, Chris Tully, et al. Working Group Report: Higgs Boson. 2013.

- [39] Rohini M. Godbole, David J. Miller, Kirtimaan A. Mohan, and Christopher D. White. Jet substructure and probes of CP violation in  $V_h$  production. *JHEP*, 04:103, 2015.
- [40] Rohini Godbole, David J. Miller, Kirtimaan Mohan, and Chris D. White. Boosting Higgs CP properties via  $VH$  Production at the Large Hadron Collider. *Phys.Lett.*, B730:275–279, 2014.
- [41] K. A. Olive et al. Review of Particle Physics. *Chin. Phys.*, C38:090001, 2014.
- [42] A. Avilez-Lopez, H. Novales-Sanchez, G. Tavares-Velasco, and J.J. Toscano. Bound on the anomalous  $tbW$  coupling from two-loop contribution to neutron electric dipole moment. *Phys.Lett.*, B653:241–248, 2007.
- [43] Jacob Baron et al. Order of Magnitude Smaller Limit on the Electric Dipole Moment of the Electron. *Science*, 343:269–272, 2014.
- [44] Jonathan Engel, Michael J. Ramsey-Musolf, and U. van Kolck. Electric Dipole Moments of Nucleons, Nuclei, and Atoms: The Standard Model and Beyond. *Prog.Part.Nucl.Phys.*, 71:21–74, 2013.
- [45] Fanrong Xu, Haipeng An, and Xiangdong Ji. Neutron Electric Dipole Moment Constraint on Scale of Minimal Left-Right Symmetric Model. *JHEP*, 1003:088, 2010.
- [46] Darwin Chang, Chong Sheng Li, and Tzu Chiang Yuan. Larger neutron electric dipole moment in left-right symmetric models. *Phys. Rev.*, D42:867–870, 1990.
- [47] Krishna Kumar, Zheng-Tian Lu, and Michael J. Ramsey-Musolf. Working Group Report: Nucleons, Nuclei, and Atoms. In *Community Summer Study 2013: Snowmass on the Mississippi (CSS2013) Minneapolis, MN, USA, July 29-August 6, 2013*, 2013.
- [48] [http://www.physics.umass.edu/acfi/sites/acfi/files/slides/yks\\_higgs\\_cpv\\_2015\\_0502.pptx](http://www.physics.umass.edu/acfi/sites/acfi/files/slides/yks_higgs_cpv_2015_0502.pptx).
- [49] Bohdan Grzadkowski and Mikolaj Misiak. Anomalous  $Wtb$  coupling effects in the weak radiative B-meson decay. *Phys.Rev.*, D78:077501, 2008.
- [50] Alexander L. Kagan and Matthias Neubert. Direct CP violation in  $B \rightarrow X(s)$  gamma decays as a signature of new physics. *Phys.Rev.*, D58:094012, 1998.
- [51] D. Asner et al. Averages of  $b$ -hadron,  $c$ -hadron, and  $\tau$ -lepton properties. 2010.
- [52] Michael Benzke, Seung J. Lee, Matthias Neubert, and Gil Paz. Long-Distance Dominance of the CP Asymmetry in  $B \rightarrow X_{s,d} + \gamma$  Decays. *Phys.Rev.Lett.*, 106:141801, 2011.
- [53] J.P. Lees et al. Measurements of direct CP asymmetries in  $BX_s$  decays using sum of exclusive decays. *Phys.Rev.*, D90(9):092001, 2014.